Underground Mining Technology 2020 - J Wesseloo (ed.)

doi:10.36487/ACG_repo/2035_20

Rock property determination

I Gray *Sigra Pty Ltd, Australia*

Abstract

Mining projects vary greatly in their location and rock properties. Despite this, the testing processes used to determine how they will behave geotechnically have become remarkably similar and more of a rote process. Test methods should be carefully tailored to suit all the possible behaviours of the rock mass. In underground mining, the properties of the underground structure are inherited rather than specified, and need to be determined. Usually, parts of the underground structure are required to collapse to yield ore, while others need to resist all manner of deformation and remain safely open. This paper reviews useful testing techniques with a particular focus on measuring what is appropriate for the situation. The paper starts by presenting some new ways of looking at uniaxial testing and the use of some simple tests to measure tensile and shear strength. It reviews the measurement of anisotropy, linear and non-linear elasticity, poroelasticity, plasticity and the multiple forms of failure. These include shear failure and tensile failure. Some of the questions surrounding anisotropy are reconsidered. Finally, the paper looks at how these measurements may be used.

Keywords: *rock properties, rock testing, rock stiffness, sheaFeqr strength, tensile strength*

1 Introduction

Any engineering design relies on an understanding of material properties. In the case of man-made materials, these properties are measured, usually to some standard, and are available for use in the design process. The tolerance on the properties is frequently quite limited. However, when dealing with natural materials such as rock, the process is not one of specifying the material, but of determining what properties the material have. To do this fully may be a very complex process as rocks typically exhibit elastic non-linearity, sometimes plasticity and frequently anisotropy. The anisotropy may be of both pre-failure behaviour and of the failure strength. In rocks, there is a need to also consider inhomogeneity. This can sometimes be described by variations in test sample properties but more generally needs to be determined by observation in the field, in bore core, or in borehole geophysics, in combination with laboratory measurements.

As not all the material properties may be relevant to a particular design, there may not be a need to measure everything, just those that are important.

The actual testing process used in rocks is frequently one that can be performed readily, rather than one which measures an absolute property. The most obvious case of this is a point load test which leads to failure at some load. However, the actual loading is a complex state of compression and tension and hence shear. The precise state of stress cannot be defined because it depends on the shape of the sample and the sample properties, which are unknown. Such tests are index tests, rather than tests that produce fundamental properties of the rock. Another example of this is the Brazilian test which is purported to measure tensile strength.

While some tests should measure fundamental properties, a failure to examine the results properly may mean that the results that are generally presented miss many aspects of the actual rock behaviour. A typical example of this is the uniaxial compression test which is reported in terms of a failure strength, Young's modulus and Poisson's ratio. Here the uniaxial compressive strength is the least likely measurement to be in error, though it should be appreciated that it is only the strength in one direction. Rock fabric such as bedding or schistosity may mean that the strength in another direction is quite different. The Young's modulus is also only measured in the axis of the core sample and may vary by several folds depending on the stress level.

Poisson's ratio measured using uniaxial loading is also likely to be stress dependent. In uniaxial loading, it typically has values that tend to be far higher than if the rock were confined in any way.

In this paper, we consider some of the test methods used by the author. Some of these are variants of standard tests that are well known, others are adaptations of existing tests and others have been developed within Sigra Pty Ltd. Those considered are:

- Measurements of rock deformation with load:
  - Uniaxial compression test.
  - Triaxial compression test.
  - Hydrostatic test.
  - Tensile tests.
- Measurements of rock strength at failure:
  - Uniaxial compression test.
  - Triaxial compression test.
  - Tensile tests.
  - Simple shear tests.
  - GOST shear test (modified).
- Included in those that measure failure are the following three index tests:
  - Brazilian test.
  - Point load test.
  - Protodyakanov test.

Figure 1 shows the loadings imposed on the rock by each of the test processes in a shear stress versus normal stress plot. Superimposed on this are the Mohr circles and Mohr–Coulomb failure envelope.

In this, the uniaxial test is shown at failure with Mohr's circle just touching the Mohr–Coulomb failure envelope. The triaxial test is also shown in a similar manner but in this case, the minor stress is not zero. A plain tensile test is also shown. It is similar to the uniaxial compression test except that the load is tensile rather than compressive.

Also shown is a Mohr's circle which represents the group of index tests which lead to failure, but in which the stress loading characteristics are not well defined. These include the Brazilian test (Ulusay & Hudson 2007), the point load test (ASTM 2007) and the Protdyakanov test. These all use compressive loading to generate tensile stress. The tensile stress is brought about by the point or line compressive load and the shape of the specimen.

In the case of the Brazilian test, the line load on a cylinder of rock generates tensile stress within it. This tensile stress may be calculated for a linearly elastic sample. However, most rock is not sufficiently linearly elastic to enable this approximation to be valid. Examination of many Brazilian test results shows that the rock has actually sheared – presumably as a result of combined tensile and compressive loading.

The point load test acts similarly to generate tensile stress by a compressive point load. Its analysis is however even more complex than that for a Brazilian test, as the geometry of the rock being tested is variable, as are its properties. Failure frequently starts by crushing of the rock below the indentation point followed by tensile, or combined shear and tensile failure. The point load test may be valuably used to test rock strength in different directions of loading.

The Protodyakanov test is used in Russia, other Commonwealth of Independent States states, and China. It involves impact which generates tensile stress in rock lumps and hence fragmentation. It is reported as an index value.

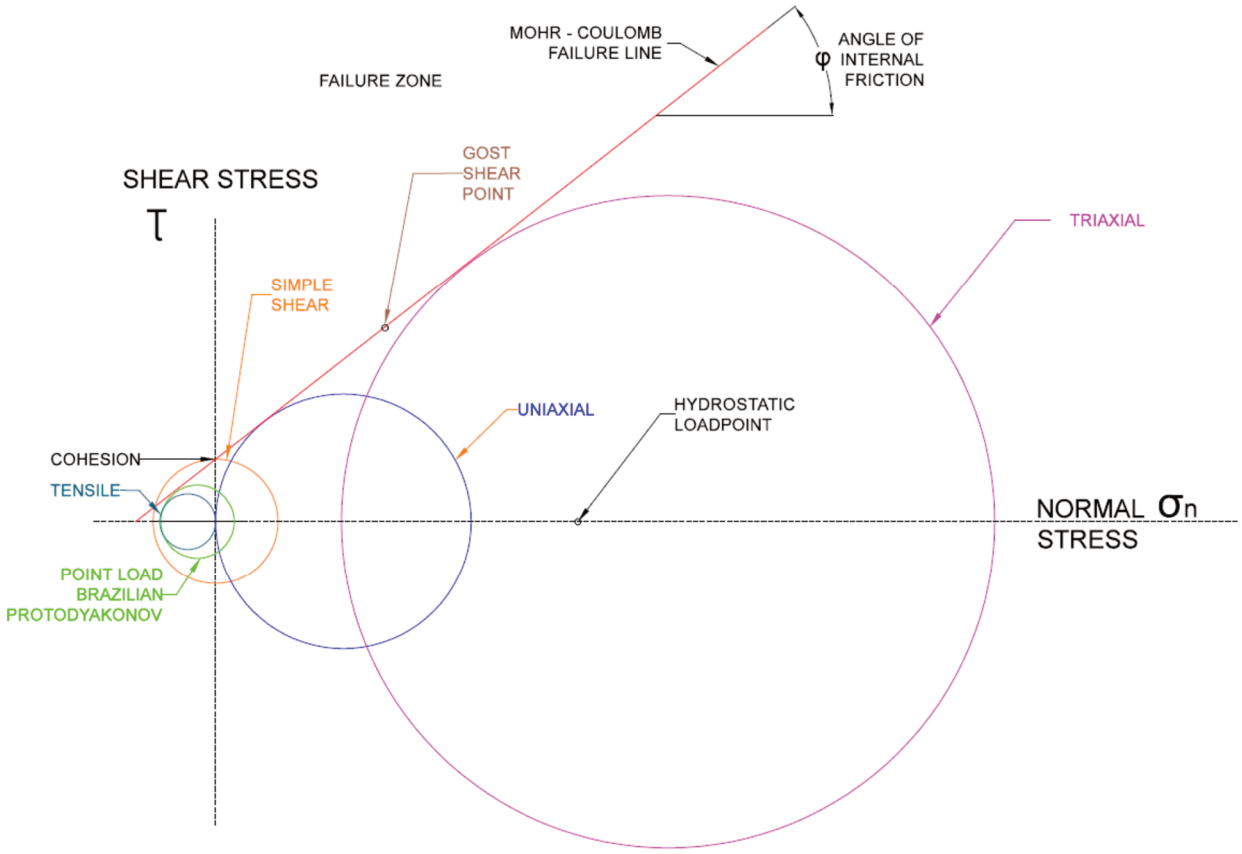

Figure 1 Stress loadings imposed by various rock tests

Also shown in Figure 1 is the loading state of the GOST shear test at failure. This is shown as a point on the Mohr–Coulomb failure line. The reason for this presentation is that the normal stress and the shear stress are directly known from measurement. A Mohr's circle could be drawn through this point. Also shown is the point associated with hydrostatic loading. This remains a point that may move along the x-axis with stress and will never generate shear stress or tensile stress leading to failure. The simple shear is not shown intersecting the failure line because it considers shear on a plane without normal stress.

All the tests shown in Figure 1, except the hydrostatic loading case, may be used to drive the sample to failure. However, only the uniaxial, tensile, GOST shear, and triaxial tests have a reasonably well-defined stress state. The point load, Brazilian, and Protodyakanov tests do not.

2 Stress and strain

Figure 2 shows a cube subject to complex stresses. Here, the first subscript of the stress tensor refers the vector perpendicular to the plane under stress (red arrow) while the second tensor subscript refers to the direction of the stress tensor (black arrow). The blue arrows are traction vectors of force on each plane.

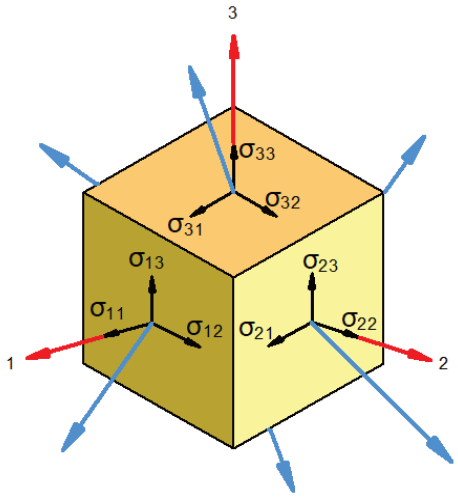

Figure 2 Cube under loading by a complex stress state

We can relate the state of stress and strain within a solid linearly elastic body by Equation 1:

$$\{\varepsilon_{ij}\} = [C_{ijkl}]\{\sigma_{kl}\} \tag{1}$$

where:

$\{\varepsilon_{ij}\}$ = a vector of strains which represents the elements of a symmetric matrix.

$\{\sigma_{kl}\}$ = a vector of stresses which represents the elements of a symmetric matrix.

$[C_{ijkl}]$ = the compliance matrix that relates stress and strain.

The compliance matrix is made up of functions of Young's moduli and Poisson's ratios and has 36 components that reduce to 21 through symmetry. Practically, this is too many components to measure and it may be reduced to nine orthotropic values if some assumptions are made. One of these is that shear does not lead to dilation. The elastic orthotropic relation, using engineering strain, is given in Equation 2.

$$\begin{Bmatrix} \varepsilon_{11} \\ \varepsilon_{22} \\ \varepsilon_{33} \\ \gamma_{23} \\ \gamma_{31} \\ \gamma_{12} \end{Bmatrix} = \begin{bmatrix} \frac{1}{E_1} & -\frac{\nu_{21}}{E_2} & -\frac{\nu_{31}}{E_3} & 0 & 0 & 0 \\ -\frac{\nu_{12}}{E_1} & \frac{1}{E_2} & -\frac{\nu_{32}}{E_3} & 0 & 0 & 0 \\ -\frac{\nu_{13}}{E_1} & -\frac{\nu_{23}}{E_2} & \frac{1}{E_3} & 0 & 0 & 0 \\ 0 & 0 & 0 & \frac{1}{G_{23}} & 0 & 0 \\ 0 & 0 & 0 & 0 & \frac{1}{G_{31}} & 0 \\ 0 & 0 & 0 & 0 & 0 & \frac{1}{G_{12}} \end{bmatrix} \begin{Bmatrix} \sigma_{11} \\ \sigma_{22} \\ \sigma_{33} \\ \tau_{23} \\ \tau_{31} \\ \tau_{12} \end{Bmatrix} \tag{2}$$

where:

E_i = represents the Young's modulus in the i direction.

ν_{ij} = represents Poisson's ratio of negative *j* direction strain divided by *i* direction strain under uniaxial loading in the *i* direction.

G_{ij} = represents the shear modulus between the *i* and *j* planes.

The orthotropic solid conveniently ignores 12 off-diagonal terms of the 21 in the full compliance matrix thus leaving nine independent terms.

In a further simplification, the orthotropic matrix may be reduced to an isotropic case in which case, all the values of Young's moduli are equal, as are all the values of Poisson's ratio. In this isotropic case, the shear modulus is expressed in Equation 3:

$$G = \frac{E}{2(1+\nu)} \tag{3}$$

It should be noted that the shear modulus terms of the orthotropic case, G_{ij}, are independent and the approximation of Equation 4 for the orthotropic case proposed by Huber (1923) is not rigorous.

$$G_{ij} = \frac{\sqrt{E_i E_j}}{2(1+\sqrt{\nu_{ij}\nu_{ji}})} \tag{4}$$

In practical testing of rock core, it is difficult to measure the shear moduli and these are generally estimated using Equation 3.

In reality, many rocks are not linearly elastic but may be represented as being so for small incremental strains.

3 Uniaxial compressive testing

Uniaxial compressive testing is about the most common form of measurement for rock strength and deformation. In its simple form, it just involves compressing a piece of core until failure occurs. If axial deformation is measured, it is possible to determine Young's modulus in the axial direction (E_1). If measurements of lateral deformation are made, then it is possible to determine Poisson's ratios ν_{12} and ν_{13}.

Figure 3 shows the results of cyclic uniaxial loading of a sandstone specimen. The x-axis shows the strains: axial positive and circumferential negative. The y-axis shows the axial stress.

This shows that the rock shows permanent offset after each load cycle. It is interesting to note that the circumferential permanent offset strain is greater than the axial permanent offset strain. This is normally the case. It also shows that the rock behaves in a highly non-linear manner. It is useful to separate the permanent offset behaviour from 'elastic' deformation. The means for doing this is shown in the Appendix.

Young's modulus is generally reported in terms of a modulus at mid-failure stress. This can be either the secant modulus or the tangential modulus. In rocks with non-linear properties, these are different but are related mathematically. This relationship is shown in the Appendix.

It should be remembered that uniaxial testing is just that: it only involves loading in one direction. Therefore, the values of modulus and Poisson's ratio only apply to that loading situation. The Poisson's ratio derived from uniaxial testing frequently reflects the effect of the permanent circumferential offset being much higher than the axial one, thus giving a false elastic Poisson's ratio.

Uniaxial testing is usually conducted on drill core. Thus, the core orientation is determined by that of the drill hole. If the rock is anisotropic, such as in laminated sedimentary material, then the relative orientation between the drill hole and the planes of weakness (bedding or schistosity) within the rock matters.

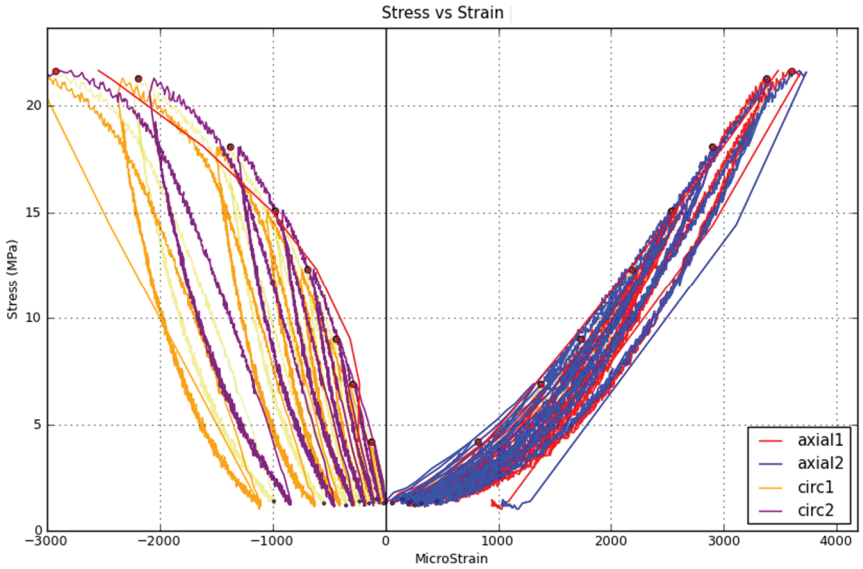

Figure 3 Results of cyclic uniaxial loading of a sandstone specimen

In analysing a cyclic loading uniaxial test, it is useful to pick the strains at the start of the loading cycle, the peak load and at the end of the loading cycle. These picks are shown schematically in Figure 4. Here, the axial strains are shown to the right and the circumferential strains are shown to the left. In this, it can be seen that the slope of the secant drawn between points A and B represents the loading secant modulus as does the slope between points C and D. The slope of the straight line between points B and C represents the unloading secant modulus. The permanent offset from the full loading cycle A-B-C is the difference in strain between points A and C. The circumferential behaviour may be analysed similarly.

The concept of a form of circumferential modulus, *A*, is useful here. *A* is the slope of the axial stress versus circumferential deformation. The secant loading values of *A* in Figure 4 are the slopes of the lines A–1 and 2–3. The unloading secant value of *A* is the slope of the line 1–2 while the tangent value of *A* is the slope of the line 1–3.

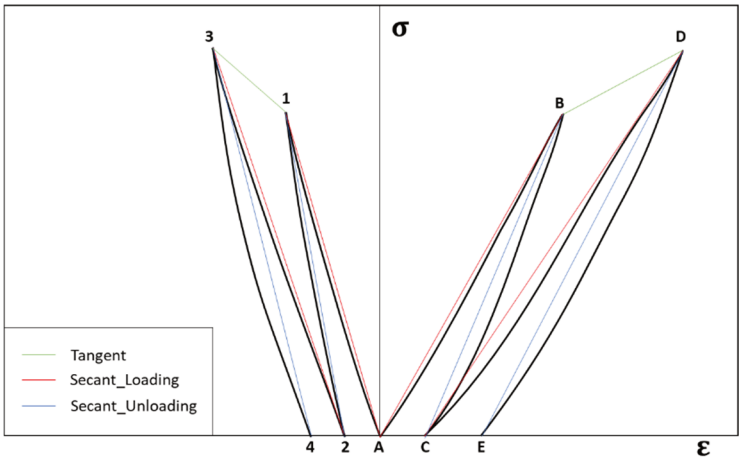

Figure 4 Picks of load and strains from a uniaxial test: schematic

Permanent deformation of the sample is an important parameter in understanding how a rock behaves. It is a useful practice to plot the total residual deformation at the end of a loading cycle versus the peak stress value achieved in the previous loading cycle. This gives a direct indication of how the sample is deforming permanently. Figure 5 shows the permanent deformation following several loading cycles. This shows that while the residual circumferential strain is initially lower than the residual axial strain, this ceases to be the case once the loading has reached 15 MPa.

This form of permanent deformation is quite characteristic of weaker sedimentary rock. It means that Poisson's ratio estimated without allowance for plastic behaviour is much larger than would otherwise be the case.

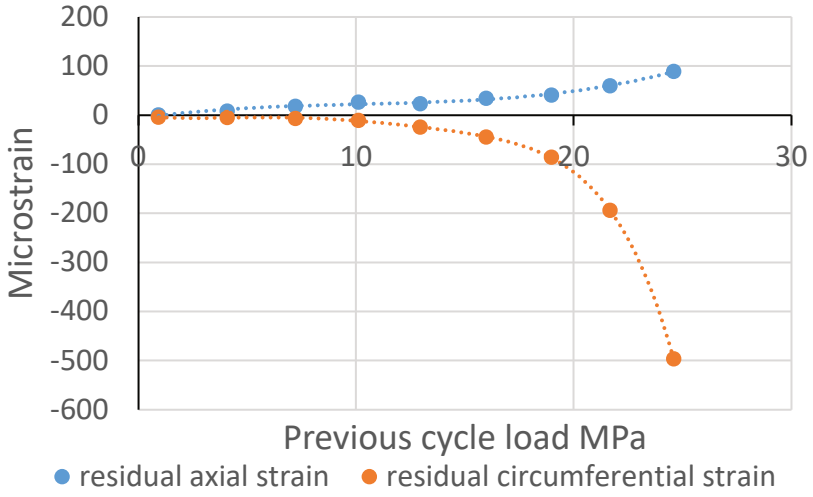

Figure 5 Residual strains following loading

There are multiple ways to determine Young's modulus and Poisson's ratio of a uniaxial test. These may be secant or tangent values and can either be corrected for the effects of permanent deformation or not. The options also exist to look at tangent values on the basis of incremental change in stress and strain, or based upon the end loads of cyclic testing.

The tangent modulus can be determined by examining the incremental changes in load and deformation. Doing this does not, however, allow for any separation of permanent deformation from the elastic component. The results may also tend to be noisy, depending on the time interval of measurement and how much filtering is applied to the data. Different loading cycles may have different shapes. The result tends to be a cloud of information on the Young's modulus and Poisson's ratio for a sample.

It is possible to reduce the amount of data to be handled by examining the end points of loading and unloading. It is also relatively straightforward to separate the effects of elastic deformation from permanent deformation. This can be done by simply subtracting the permanent deformation at the end of each loading cycle in the calculation of a mean secant modulus. Doing this for the cases of loading shown in Figure 4 leads to Equation 5:

$$E_{sae} = \frac{2\sigma_B - \sigma_A - \sigma_C}{2(\varepsilon_B - \varepsilon_{C)}} \quad (5)$$

where:

E_{sae} = the mean axial secant modulus evaluated at stress σ_B with the effect of permanent deformation having been removed.

All the strains used in Equation 5 are axial strains.

By a similar procedure, it is possible to arrive at a similar equation for the secant circumferential modulus, *A*. This is shown in Equation 6:

$$A_{sae} = \frac{2\sigma_B - \sigma_A - \sigma_c}{2(\varepsilon_1 - \varepsilon_{2)}} \quad (6)$$

There is a direct mathematical relationship between the secant modulus and the tangent modulus. This is developed in the Appendix and summarised in Equation 7:

$$E_{Ta} = \frac{d}{d\varepsilon}(E_S)_a + E_{Sa} \tag{7}$$

where:

E_{Ta} = the tangent modulus at point *a.*

$\frac{d}{d\varepsilon}(E_S)_a$ = the derivative of the secant modulus with respect to strain evaluated at point *a.*

E_{Sa} = is the secant modulus evaluated at point *a.*

An equation of the same form as Equation 7 can also be applied to develop a tangent circumferential modulus. Figure 6 is derived from Figure 4. It shows the mean stress and strain endpoints for the axial and circumferential strain versus stress.

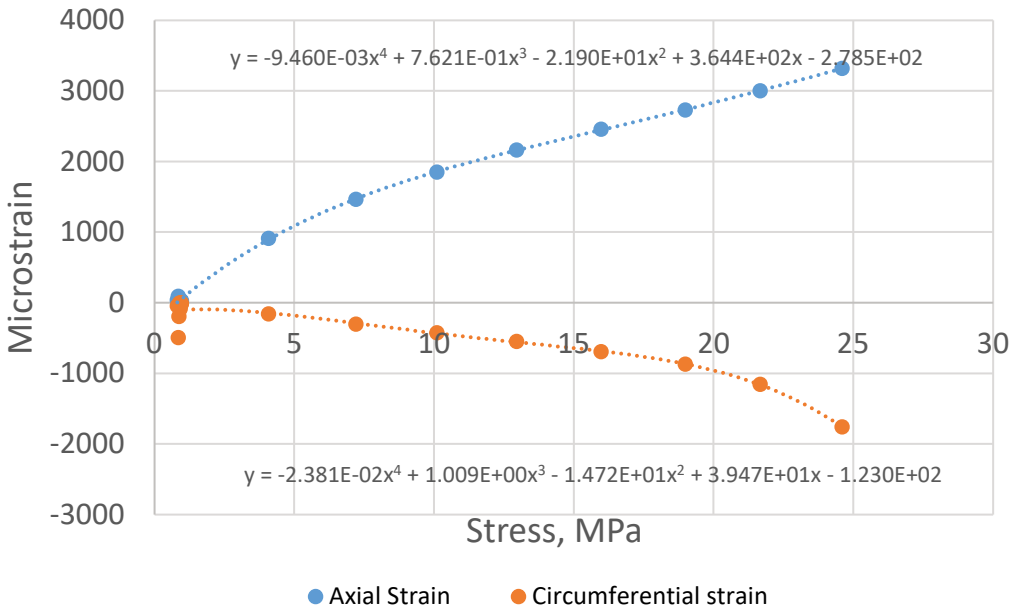

Figure 6 Endpoints of stress and strain from cyclic loading cases

Using the data presented in Figure 6, we can now calculate the following forms of Young's modulus:

1. The direct secant loading modulus without correction for permanent offset.
2. The direct secant unloading modulus without correction for permanent offset.
3. The average secant modulus with correction for permanent offset.
4. The tangent modulus, as per Equation 7, with a correction for permanent offset.
5. The direct tangent modulus without correction for permanent offset.

These are presented in Figure 7. The legend is in the same order as the cases above. As can be seen, the secant Young's moduli for loading, unloading and mean (corrected for permanent offset) cases are almost identical. The tangent moduli are similar until the higher stresses when permanent offset makes the one derived with a correction for permanent offset a bit higher in value. The tangent moduli are significantly different from the secant ones. This is a function of the non-linearity of the sample behaviour.

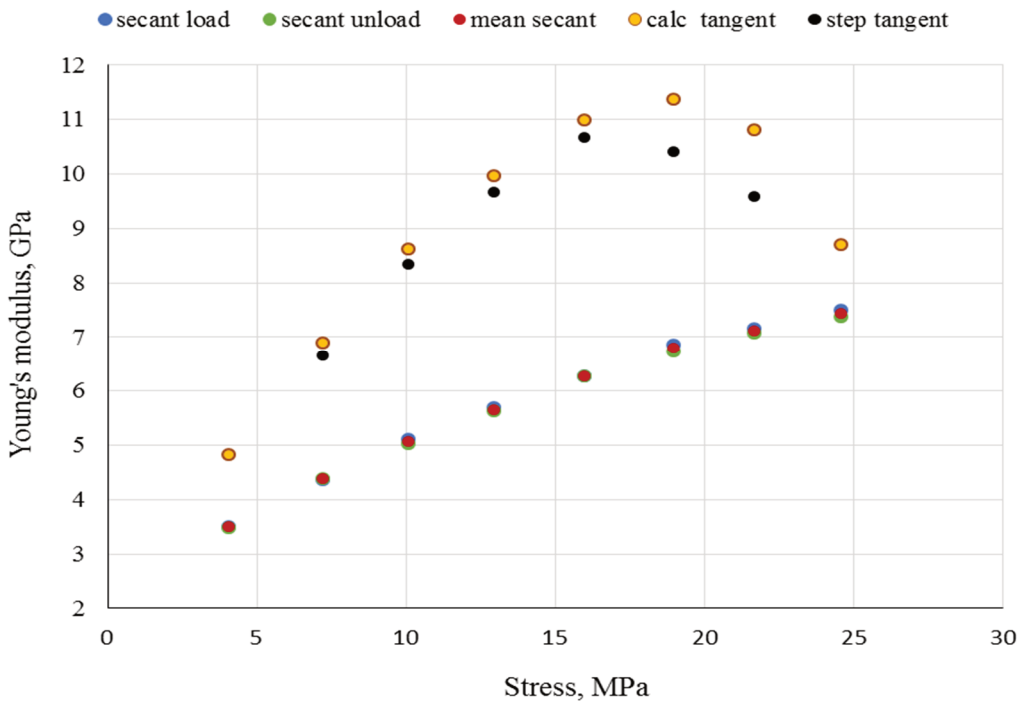

Figure 7 Plots of Young's moduli versus stress derived from the same uniaxial test

If we calculate Poisson's ratio as the negative ratio of the Young's modulus divided by the circumferential modulus, *A*, in the different forms, then we get the following cases:

1. The direct loading secant value of Poisson's ratio without correction for permanent offset.
2. The direct unloading secant value of Poisson's ratio without correction for permanent offset.
3. The mean secant value of Poisson's ratio with correction for permanent offset.
4. The calculated value of tangent Poisson's ratio with correction for permanent offset.
5. The direct tangent value of Poisson's ratio without correction for permanent offset.

These are shown in Figure 8 with the legend being in the same order as the cases above.

There is a small difference between the loading and unloading secant cases. This becomes more pronounced at higher stresses when offset strains get higher. The mean secant modulus is very close to the unloading secant case. The calculated tangent is based on the approach of Equation 7 using data corrected to remove permanent offset. The case of real note is that of the simple tangent values of Poisson's ratio with no correction for permanent offset. These increase rapidly with stress as the permanent offset component of their value becomes greater. When calculated in this form, the tangent Poisson's ratio becomes more of an indicator of permanent offset and hence, the approach of failure, than anything else.

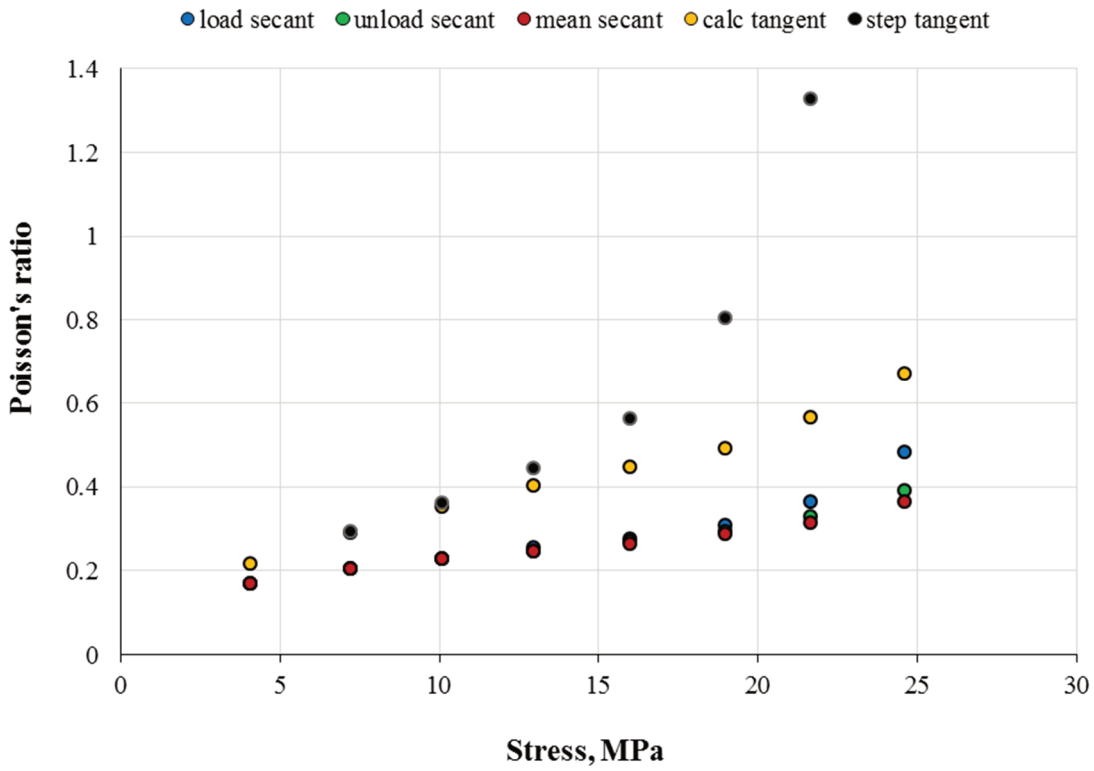

Figure 8 Poisson's ratios calculated by various methods

Uniaxial test rock properties are normally reported at half the failure stress. In this case, the secant Young's modulus and Poisson's ratio would normally be reported as 5.4 GPa and 0.25. In reality, the range of the secant Young's modulus is 3.5 to 7.4 GPa while that for the secant Poisson's ratio is 0.15 to 0.40.

In the case of the tangent properties, the reported Young's modulus would be 9.5 GPa compared to a range of 2.5 to 11.4, depending on the method of calculation. The value of Poisson's ratio that would be reported is 0.44 whereas if it were to be calculated properly, it could lie somewhere between 0.5 and 0.33. These are very big differences and it is necessary to look at the data and ask how the values are arrived at. Also, most importantly, the question should be asked as to what it means in the context of the rock mechanics problem being considered? It is certainly not possible to say that most sedimentary rock has a specific value of modulus. Frequently, it is not possible to get a sensible value of Poisson's ratio out of a uniaxial test and recourse should be made to a triaxial test, as quite a small degree of confinement can dramatically reduce the apparent value of Poisson's ratio.

The cases presented above are for a medium-grained sandstone which is quite non-linear and exhibits some permanent offset. It is, however, quite testable. Figure 9 presents a typical stress–strain plot for coal. It is non-linear, exhibits huge permanent offset, and starts to fail at a very low stress because of lack of confinement. This plot exemplifies the difficulties in uniaxial testing of coals, and for that matter weaker rocks, in the hope that it is possible to get sensible values of Young's modulus and Poisson's ratio. Frequently, the only piece of coal that can be tested is totally unrepresentative of the rest of the coal seam.

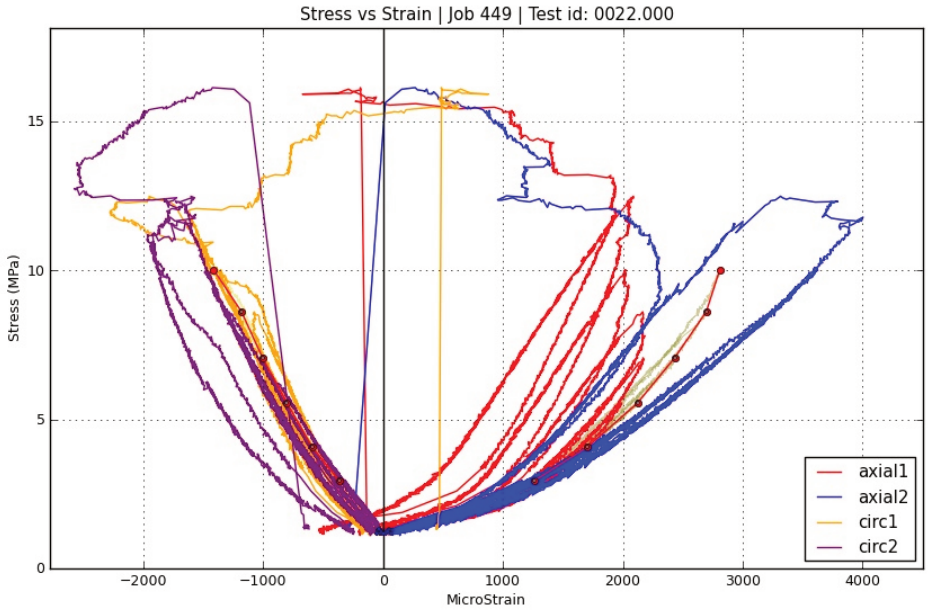

Figure 9 Plot of axial and circumferential strains versus axial stress for a typical coal sample

4 Triaxial compressive testing

The triaxial compressive test is normally used to determine failure strength under axial loading of core with a confining loading applied to it through an elastomeric sleeve. The Hoek cell (Hoek & Franklin 1968) is commonly used for this purpose. Sometimes, the deformation associated with triaxial loading is measured using strain gauges. In this case, it is possible to determine deformation under triaxial loading conditions. This is seldom fully analysed and in the case of the Hoek cell, it is difficult to apply a higher confining load than axial load.

The mode of failure that occurs under a normal triaxial test on intact rock core is invariably one of diagonal shear through the core. As in the uniaxial test case this failure mode may not represent what will occur in the rock mass, where failure is likely to be on preferential planes of weakness such as bedding planes or schistosity. The measurements gained from this test process are therefore limited by the geometry of the core hole from which the sample is taken and its relative orientation compared to the planes of weakness. If the core is obtained from a vertical hole crossing horizontal bedding planes then the triaxial failure parameters will bear little relation to a failure that may occur on the bedding plane.

Triaxial testing with careful measurement of deformation may, however, be used to great advantage to obtain the elastic properties of the rock. Gray et al. (2018), describe the measurement of Young's moduli, Poisson's ratios and the poroelastic coefficients of sedimentary rock. These have generally been found to be quite non-linear and frequently have significant anisotropy. The Young's modulus measured parallel to the bedding planes is typically up to two times that measured perpendicular to the bedding. On occasions the lateral modulus, E_2or E_3 is found to be four times the axial modulus E_1. This is a huge difference and strongly affects the behaviour of the rock under loading. Such differences cannot be ignored in numerical analysis of the behaviour of a rock mass.

Figure 10 shows an example of the varying axial Young's modulus (E_1) for a Hawkesbury sandstone from the Sydney area. This is a highly non-linear rock with a four-fold change in Young's modulus in 20 MPa stress range. The axial Young's modulus (across the bedding planes) is shown here to be primarily controlled by the axial stress. In this specimen, the transverse Young's modulus was primarily controlled by the confining stress. The specimen behaviour was reasonably isotropic. Not all samples behave this way. In many, the Young's moduli are a function of the axial and confining stress. This is thought to be due to the granular structure and matrix of the rock.

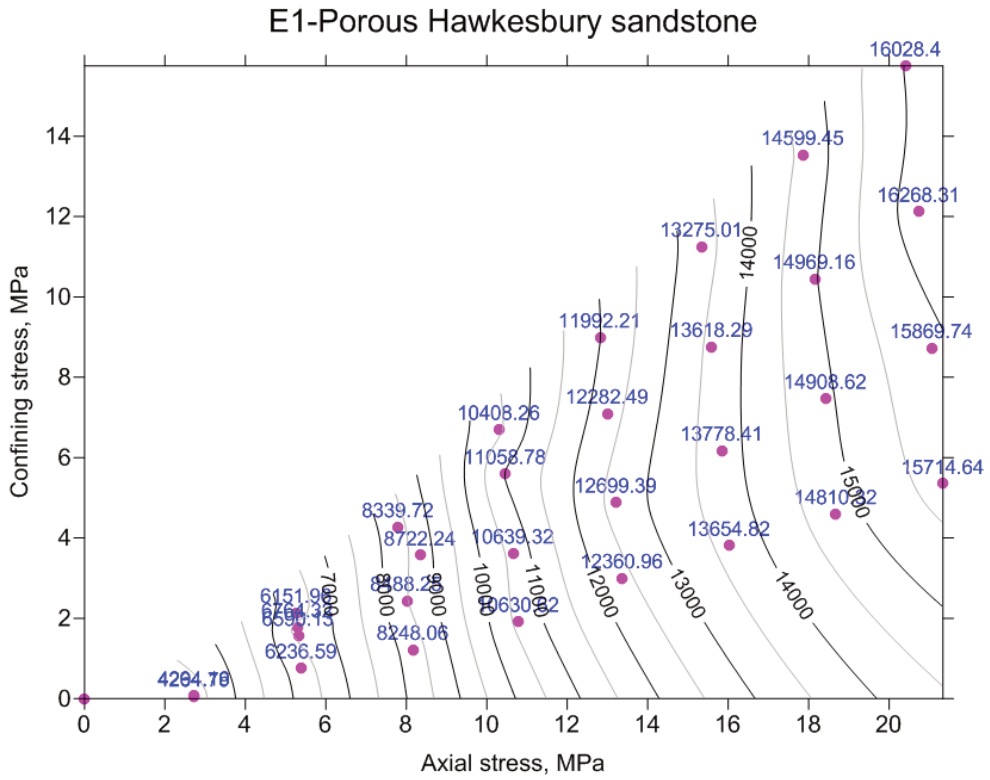

Figure 10 Axial (E_1) Young's modulus for a Hawkesbury sandstone

Poroelastic behaviour defines how fluid pressure affects the deformation of the rock. Some fraction of the fluid pressure acts as though to modify the stress within the rock mass. This effect is described by the poroelastic coefficients which are directional. If the rock lacks pore space or fractures then the coefficients are zero. If the rock has a large and fixed pore space, the coefficients may approach unity as is the case with a soil. In the case of rock containing small, partially closed fractures, the poroelastic value increases as the fractures open. It is also quite directional depending on fracture orientation.

5 Hydrostatic testing

The hydrostatic test was originally developed by the author's company as a means to determine the elastic properties of coal samples that disintegrated on retrieval due to the effects of desorbing gas. It provided a means to measure the elastic properties of fragments. The test method has been developed further and is now used to measure any odd shaped specimen such as that from a stress measurement overcore operation.

The test process involves fitting strain gauge rosettes to a piece of rock, casting it in a soft elastomer and then placing the sample in a water filled pressure vessel. The sample is then loaded in a sequence of steps and the strains measured. An example of a test specimen is shown in Figure 11. The test method is described in more detail in Gray et al. (2018).

On its own, the test method cannot provide a complete solution to the stress strain behaviour of the rock. If the rock is linear and one Young's modulus is known, then it is possible to derive the other moduli and the Poisson's ratios using an assumption that the rock behaves in an orthotropic manner. Alternatively, if an estimate of a mean Poisson's ratio can be made then the Young's moduli and Poisson's ratios may be derived from the test. Where the rock's Young's moduli and Poisson's ratios vary with the state of stress, it is not possible to separate these, however, useful comparative values may be obtained.

The test method is particularly useful in dealing with odd shaped fragments and in determining the relative Young's moduli in different directions. Because of the nature of loading, no shear or tensile stress is generated and therefore, the method is unsuitable for measuring rock strength.

Figure 11 Strain gauged sample of phyllite cast in silicone resin for hydrostatic testing

6 Axial tensile test

This test is used to measure the tensile strength of core to axial loading. It follows ASTM (2020). It involves gluing tubes to each end of a piece of core and then axially loading it to failure. The results are reported in terms of tensile stress.

In homogeneous rock, the result of the test is a simple tensile strength. If conducted on core which is laminated approximately perpendicularly to the core, it provides the tensile strength across the laminations. This is particularly relevant to roof falls or caving behaviour in laminated rock.

7 Transverse tensile test

This test is used to measure the tensile strength of rock perpendicular to core. It is of particular relevance to longwall design in massive strata. Here, the tensile strength of the rock in the direction of the bedding plane in many cases determines the caving behaviour.

Tensile loading may be applied transversely to the core. To enable this, the core is cut transversely to form a biscuit of rock which is normally a quarter of the diameter (15 mm for HQ-3 sized core), as shown in Figure 12. This core biscuit is then glued between two steel plates on each side of the biscuit leaving a gap of one eighth the core diameter (8 mm for HQ-3 core) in between the plates. The sample is fitted into a universal test machine and the gap is monitored on each side by strain gauged C rings, as shown in Figure 13. The core biscuit is then loaded via these plates using a load balancing system side plate and the load versus deformation value determined.

Almost invariably, one side of the core biscuit fails before the other, due either to inhomogeneity in the rock or due to uneven loading leading to some degree of bending in the sample. The latter may be corrected by analysis of the uneven deformation of each side of the core to arrive at a more accurate tensile strength.

Figure 12 Biscuit shaped piece of core for transverse tensile test

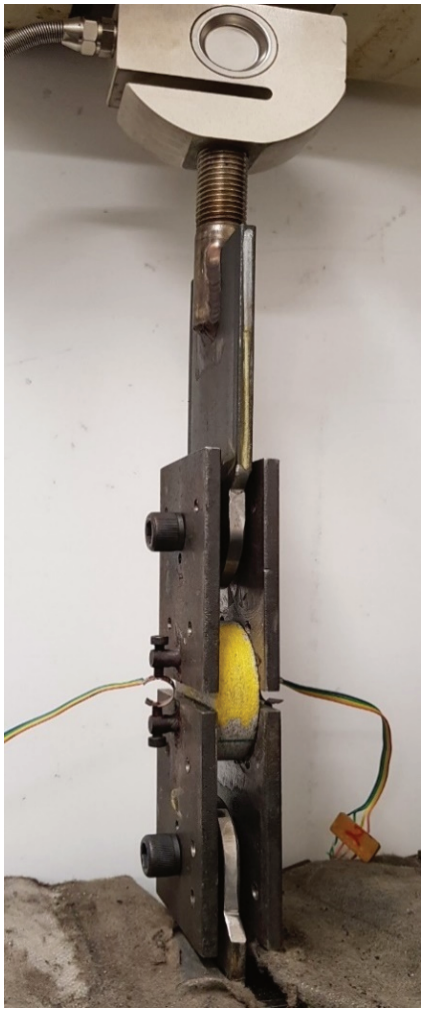

Figure 13 Test sample in universal test machine prior to failure

The transverse tensile stress at failure is calculated using the failure load, the width, and depth of the failed face. The use of C ring deformation gauges enables the transverse tensile Young's modulus to be determined and corrections made to the failure stress for any induced bending in the test process.

8 Simple shear test

This test is designed to test the shear strength of laminated core. It is particularly suited to sedimentary rocks with a weak bedding plane that is roughly perpendicular to the core. The test involves sitting the core in a double-sided saddle which is supported on a semi-spherical mount and loading it with a central inverted saddle. The upper part of the saddle is used to apply load to the sample. It is the same width as the gap in the lower portion of the saddle so that no bending moment is generated within the core. The test setup is shown in Figure 14.

Figure 14 Simple shear test setup on a laminated sandstone

Generally, one side of the core section shears before the other side, depending upon which side is the weaker, or which has a favourably aligned plane of weakness. To determine the shear strength of the core sample, half of the recorded load at failure is divided by the shear surface area to yield a shear strength. The value of shear stress corresponds to the value of cohesion on the failure plane.

The test is particularly useful when used to gain multiple values of cohesion, as one end typically breaks after each test and the core can be advanced by a short distance to enable another test to be taken. It is a quick and simple test that yields multiple values out of fairly short lengths of core.

9 Modified GOST (ГОСТ) shear test

This test is derived from the Russian standard ГОСТ (1988). It involves inserting a core into a split cavity on each side of a split cylinder. The split cylinder is then rotated to a test angle and is loaded to failure. The loading applies normal stress and shear to the plane of the core between the split cylinder and shears the rock. By shearing sequential specimens at different angles, a variety of values of shear and normal stress at failure are acquired. These may be presented on a plot of shear stress versus normal load, and the cohesion and angle of internal friction can be derived. The original standard shows the core being sheared longitudinally.

In the author's version, the core is sheared transversely. In this mode, the shear strength behaviour of bedding planes is directly measured. The test apparatus can accommodate specimens that are from 30 to 60 mm long. This enables a number of test samples to be obtained from a short length of core.

The test apparatus is shown schematically in Figure 15 and physically in Figure 16.

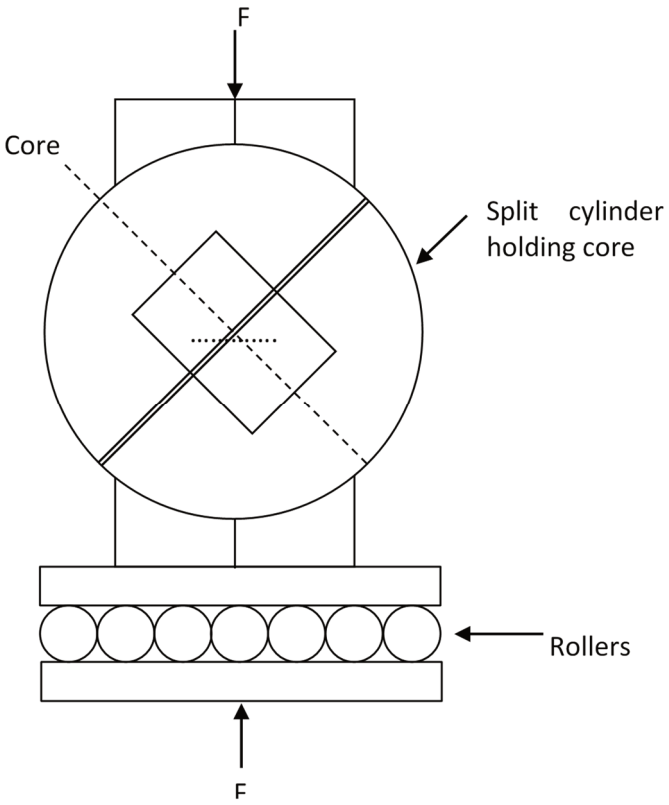

Figure 15 Schematic diagram of modified GOST shear test

Figure 16 Modified GOST shear test setup in universal test machine

Different loading angles (25°, 35°, 40° and 45° to the load direction) mean that different ratios of normal to shear stress are generated. The values of shear to normal stress may be directly calculated at failure and plotted as is shown in Figure 17.

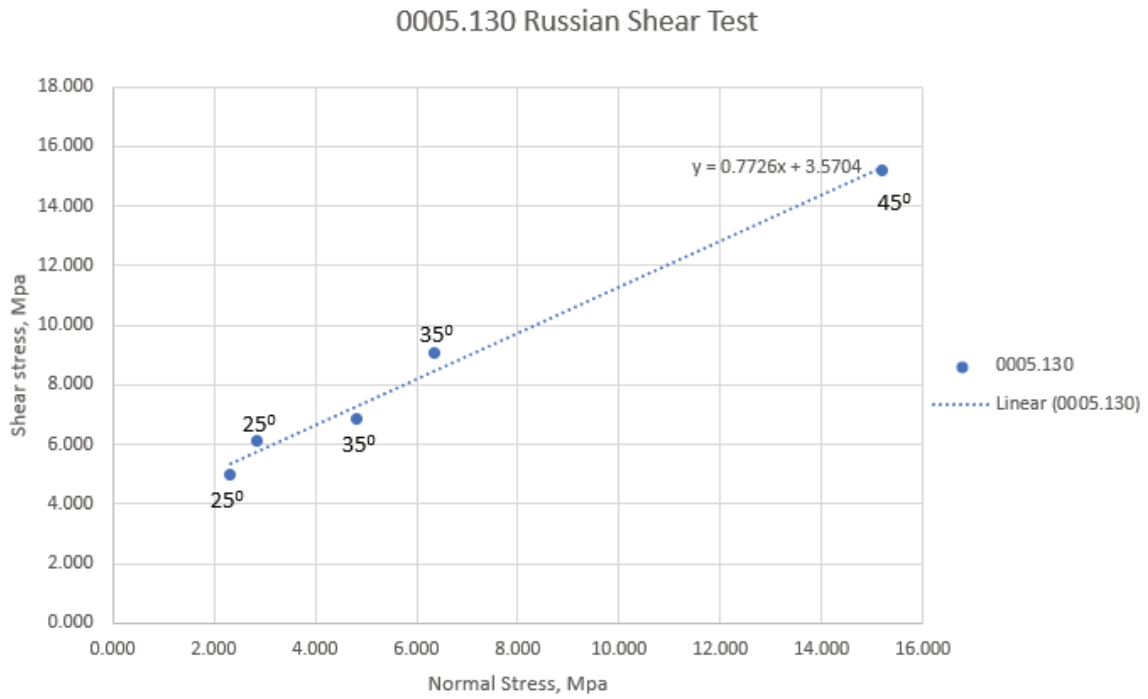

Figure 17 Shear versus normal stress at failure from modified GOST shear test

The GOST shear test is, in many ways, a development of the simple shear test which also enables normal loading across the failure plane. It is however a little more complex to set up.

10 Protodyakanov test

This test is mentioned because of its wide use in those parts of the world that came under the influence of the Soviet Union. As such, there are many references that use it. These extend from outburst risk determination to suitability of coal to hydraulic mining. It is a useful, simple test to get an idea of rock strength.

This is a test on lumps of rock. The process involves four weighed sets of rock consisting of five subsamples each with size range 20 to 30 mm. The subsample is placed in an apparatus comprising a drop hammer of 2.4 kg weight with a 600 mm travel. The diameter of the hammer is 66 mm and the tube it falls within is 76 mm. The number of hammer blows depends on rock strength and is determined experimentally. The amount of fines of less than 0.5 mm diameter is measured in a measuring cylinder (a tube of 23 mm diameter). The height of fines in the measuring tube after crushing of one set (five subsamples) should be in the range of 20–100 mm, otherwise the number of blows should be adjusted experimentally. For coal, usually one blow is enough, but for some strong coals, two to three blows are required.

The Protodyakanov drop hammer apparatus and measuring cylinder are shown in Figure 18.

The *f* coefficient is defined by Equation 8:

$$f_{20-30} = \frac{20*n}{h} \tag{8}$$

where:

f_{20-30} = the toughness index (for 20–30 mm size range).

n = the number of hammer blows.

h = the scale measurement in the cylinder after five subsample tests (mm).

The final result is an average of four measurements.

The general threshold *f* value less than 0.5 is regarded as being indicative of outburst proneness.

A Chinese extension to the test method for fine coal, where it is not possible to obtain 20–30 mm lumps, is to sieve the sample for the 1–3 mm range. This is then hammered three times and the size reduction noted by a measurement in the fines cylinder.

In this case, if $f_{1-3} > 0.25$ using Equation 8 with $n = 3$

then the equivalent $f_{20-30} = 1.57 \times f_{1-3} - 0.14.$

Otherwise if $f_{1-3} \leq 0.25$

then the equivalent $f_{20-30} \equiv f_{1-3}.$

Figure 18 Protodyakanov drop hammer apparatus (right) and measuring cylinder (left)

11 Discussion

Table 1 shows what information may be obtained from the tests discussed in this paper. These are broken into high quality measurements of directly derived parameters, those tests from which parameters may be deduced with an assumption (second quality) and those tests which are purely index tests, but which are possibly too frequently correlated with real properties. Added to the second quality level tests is the measurement of Poisson's ratio from uniaxial testing.

This table cannot show everything, for example, the importance of bedding plane or foliation on shear strength. This requires the person specifying the test to understand the reasons for performing the test. If, for example, we are expecting failure in a laminated strata, then this may be dominated by tensile failure across, or shear failure along the bedding planes. In the same strata, tensile failure may occur by bending of a unit, as in a longwall goaf, and tensile failure in the direction of the bedding plane may dominate. In massive strata the tensile strength in the direction of the bedding plane may be very large.

The nature of loading in the simple shear and modified GOST test may be criticised as it may be considered to be of a line or point nature. In fact, both tests work well when used to measure rock which is inherently weaker in the direction transverse to the core.

Table 1 Rock property testing showing the results that may be derived from the tests

Test type	Axial modulus E_1	Trans modulus E_2	Trans modulus E_3	Axial Poisson's ratio V_{12}	Geometric mean Poisson's ratio V_a	Poroelastic coefficients	Plastic deformation	Uniaxial compressive strength	Axial tensile strength	Transverse tensile strength	Cohesion C	Friction ϕ
Laboratory												
Simple uniaxial												
Cyclic uniaxial												
Simple shear												
GOST shear												
Triaxial – elastic												
Triaxial - failure												
Hydrostatic												
Transverse tensile												
Axial tensile												
Slake												
Field												
Point load												
Brazilian												
Protodyakanov												

High quality measurement	
Second quality measurement	
Derived from index test	

The Brazilian test is noted as a field test here as this is how it is used by Sigra

E_1 = Young's modulus in the axial direction of the core

E_2 = Young's modulus (minor) perpendicular to the core

E_3 = Young's modulus (major) perpendicular to the core

V_{12} = Poisson's ratio measured by axial loading of the core

C = Cohesion according to Mohr–Coulomb theory

ϕ = Friction angle according to Mohr–Coulomb theory

V_a = Geometric mean Poisson's ratio

12 Conclusions

A number of test methods have been presented in this paper. Some of these are conventional, some have been developed by the author's company, and some have come from Russian experience. Testing needs must be evaluated in terms of what is required to be measured and what can be measured. What is important is that it is of no use just doing tests because that is what has been done previously. Endless rote testing by uniaxial compression is probably useless if the design is dependent on shear strength or transverse tensile strength on a bedding plane, or by buckling on schistosity. Similarly, triaxial testing that leads to a shear failure direction that bears no relation to the expected shear failure direction in an anisotropic rock is valueless.

The proper measurement of elastic parameters is also important. It is no use setting up a numerical model that uses isotropic linear rock properties if the rock actually has a change in Young's modulus of 4:1 over the stress ranges being considered and anisotropy of 2:1. The choice of Poisson's ratio to be used is also frequently incorrect as the confined Poisson's ratio is generally much less than that measured by uniaxial testing.

The use of index tests may be immensely useful but it must be remembered that they provide measurements that are derived from a combination of loadings. They are useful for comparison not in exact design, unless of course they indicate that the design is well and truly safe or will undoubtedly fail.

Appendix: Relationship between tangent and secant Young's moduli and Poisson's Ratio from uniaxial testing

This Appendix references Figure 4 in the main body of the paper.

The tangent axial Young's modulus is defined by Equation 9:

$$E_{T1} = \frac{d\sigma_1}{d\varepsilon_1} \tag{9}$$

The secant axial Young's modulus is defined at some point *a* on the loading or unloading curve as Equation 10:

$$E_{S1a} = \frac{\sigma_{1a}}{\varepsilon_{1a}} \tag{10}$$

This can be alternatively described by Equation 11:

$$E_{S1a} = \int_0^{\varepsilon_{1a}} \frac{d\sigma_1}{d\varepsilon_1} d\varepsilon_1 / \varepsilon_{1a} \tag{11}$$

Which may be rewritten as Equation 12:

$$E_{S1a} = \int_0^{\varepsilon_{1a}} E_{T1} d\varepsilon_1 / \varepsilon_{1a} \tag{12}$$

By re-arranging Equation 12 to Equation 13:

$$\int_0^{\varepsilon_{1a}} E_{T1} d\varepsilon_1 = E_{S1a}\varepsilon_{1a} \tag{13}$$

By differentiating Equation 13 with respect to strain we get Equation 14:

$$E_{T1a} = \frac{d}{d\varepsilon_1}(E_{S1a}).\varepsilon_{1a} + E_{S1a}.\frac{d}{d\varepsilon_1}(\varepsilon_{1a}) \tag{14}$$

Re-arranging we get Equation 15:

$$E_{T1a} = \frac{d}{d\varepsilon_1}(E_{S1a}).\varepsilon_{1a} + E_{S1a} \tag{15}$$

where:

E_{T1a} = the tangent Young's modulus in the axial (1) direction at strain ε_{1a}.

E_{S1a} = the secant Young's modulus in the axial (1) direction at strain ε_{1a}.

Equation 15 describes the Tangent axial modulus in terms of the secant axial Young's modulus, its derivative with respect to strain and the axial strain at which it is being evaluated. Because the secant Young's modulus is being used the effect of an offset strain is minimised because it is spread over the entire loading strain.

Let us define a modulus type term, *A*, relating axial stress and lateral strain associated with axial stress in Equation 16:

$$A_{T2} = \frac{d\sigma_1}{d\varepsilon_2} \tag{16}$$

Then it is possible to follow identical steps as for the axial strain case and arrive at Equation 17 which is an analogue of Equation 15 only defined in terms of circumferential strain.

$$A_{T2b} = \frac{d}{d\varepsilon_2}(A_{S2b}).\varepsilon_{2b} + A_{S2b} \tag{17}$$

where:

A_{T2b} = the tangent value of axial stress with respect to circumferential strain at strain level b.

A_{S2b} = the secant value of the axial stress with respect to circumferential strain at strain level b.

The tangent value of Poisson's ratio is defined in Equation 18 in which the values of the tangent Young's modulus and the tangent value of A are evaluated at the same axial stress level.

$$v_{T12} = -\frac{d\varepsilon_2}{d\varepsilon_1} = -\frac{\frac{d\sigma_1}{d\varepsilon_1}}{\frac{d\sigma_1}{d\varepsilon_2}} = -\frac{E_{T1a}}{A_{T2b}} \tag{18}$$

The secant Poisson's ratio is simply the negative ratio of the circumferential to axial strain associated with total loading or unloading as in Equation 19:

$$v_{S12} = -\frac{\varepsilon_2}{\varepsilon_1} \tag{19}$$

The process to determine the tangent axial Young's modulus and the tangent Poisson's ratio is as follows:

1. Cyclically load the sample.
2. Plot the load and strain data on a time base.
3. Pick the load and strain for the initial unloaded case.
4. Pick the load and strain for the full load case.
5. Repeat 3 and 4 until the end of the test. This is usually at the failure of the sample.
6. Calculate the unloading cases of the secant Young's modulus E_{S1} for each load cycle.
7. Calculate the unloading cases of the secant value of A_{S2} for each load cycle.
8. Plot the values of the unloading E_{S1} and A_{S2} for each cycle.
9. Fit a simple differentiable function to each of the cases being considered. This could be a linear equation, a more complex polynomial, or a cubic spline.
10. Solve Equation 15 for the tangential Young's modulus E_{T1}.
11. Solve Equation 17 for the tangential value of A_{T2}.
12. Solve Equation 19 for the tangential Poisson's ratio.

References

ASTM 2007, *D5731-07 Standard Test Method for Determination of the Point Load Strength Index of Rock and Application to Rock Strength Classification*, ASTM International, West Conshohocken.

ASTM 2020, *D2936-20 Standard Test Method of Direct Tensile Strength of Intact Rock Core Specimens*, ASTM International, West Conshohocken.

ГОСТ (Gost) 1988, *21153.5-88 Method for the Determination of Rock Shear Strength Under Compression*, USSR State Publisher.

Gray, I, Zhao, X & Liu, L 2018, 'The determination of anisotropic and nonlinear properties of rock through triaxial and hydrostatic testing', *Proceedings of the 10th Asian Rock Mechanics Symposium*, International Society for Rock Mechanics and Rock Engineering, Lisbon.

Hoek, E & Franklin, JA 1968, 'A simple triaxial cell for field and laboratory testing of rock', *Transactions of the Institution of Mining and Metallurgy,* vol. 77, pp. A22–A26.

Huber, M 1923, 'The theory of crosswise reinforced ferroconcrete slabs and its application to various important constructional problems involving concrete slabs', *Der Bauingenieur 4*, vol. 12, pp. 354–360.

Ulusay, R & Hudson, HA 2007, *The Complete ISRM Suggested Methods For Rock Characterization, Testing And Monitoring: 1974–2006*, ISRM Turkish National Group, Ankara.